

The SkipSponge Attack: Sponge Weight Poisoning of Deep Neural Networks

Jona te Lintelo
Radboud University
the Netherlands
jona.telintelo@ru.nl

Stefanos Koffas
Delft University of Technology
the Netherlands
s.koffas@tudelft.nl

Stjepan Picek
Radboud University
the Netherlands
Delft University of Technology
the Netherlands
stjepan.picek@ru.nl

ABSTRACT

Sponge attacks aim to increase the energy consumption and computation time of neural networks deployed on hardware accelerators. Existing sponge attacks can be performed during inference via sponge examples or during training via Sponge Poisoning. Sponge examples leverage perturbations added to the model's input to increase energy and latency, while Sponge Poisoning alters the objective function of a model to induce inference-time energy effects.

In this work, we propose a novel sponge attack called SkipSponge. SkipSponge is the first sponge attack that is performed directly on the parameters of a pre-trained model using only a few data samples. Our experiments show that SkipSponge can successfully increase the energy consumption of image classification models with fewer samples required than Sponge Poisoning. We show that poisoning defenses are ineffective if not adjusted specifically for the defense against SkipSponge (i.e., they decrease target layer bias values). Our work shows that SkipSponge is more effective on the GANs and the autoencoders than the state-of-the-art. Additionally, SkipSponge is stealthier than the previous Sponge Poisoning attack as it does not require significant changes in the victim model's weights. Our experiments indicate that the SkipSponge attack can be performed even when an attacker has access to only 1% of the entire dataset and reaches up to 13% energy increase.

KEYWORDS

Sponge Poisoning, Availability Attack, Image Classification, GAN, Autoencoder

ACM Reference Format:

Jona te Lintelo, Stefanos Koffas, and Stjepan Picek. 2024. The SkipSponge Attack: Sponge Weight Poisoning of Deep Neural Networks. In *Proceedings of ACM Conference (Conference'17)*. ACM, New York, NY, USA, 16 pages. <https://doi.org/10.1145/nnnnnnn.nnnnnnn>

1 INTRODUCTION

The wide adoption of deep learning models in production systems introduced a variety of new threats [22]. Most of these threats target

the model's confidentiality and integrity. Evasion attacks [46] alter the model's input to produce wrong results targeting the model's integrity. Additionally, backdoor attacks insert a secret functionality into a trained model that can be activated at inference time, affecting mostly the model's integrity [12]. Model stealing [18], membership inference [43], and model inversion [10] attacks extract private information from a trained model violating the victim's confidentiality. The model's availability was initially violated by the untargeted poisoning attack that caused a denial of service by significantly decreasing the model's performance. However, recently a new category of attacks that target the model's availability has been introduced, sponge attacks [8, 39, 42, 44]. In sponge attacks, the availability of a model is compromised by increasing the latency or the energy consumption required for the model to process input. Energy considerations for deep neural networks are highly important. Indeed, numerous papers report that the energy consumption for modern deep neural network models is huge, easily being megawatt hours, see, e.g., [37, 38, 41].

Increasing the models' latency and energy consumption is possible when neural networks are deployed in application-specific integrated circuit (ASIC) accelerators. ASIC accelerators are used in research and industry to improve the time and cost required to run Deep Neural Networks (DNNs) [2, 28]. More specifically, neural networks are deployed on sparsity-based ASIC accelerators to reduce the amount of computations made during an inference pass. Sponge attacks leverage the reduction of sparsity to eliminate the beneficial effects of ASIC accelerators.

As first shown by Shumailov et al. [44], the availability of models can successfully be attacked through sponge attacks. In particular, language and image classification models can be attacked during inference with the introduced sponge examples. Sponge examples are maliciously perturbed images that require more energy for inference than regular samples. This attack greatly increases the energy consumption on the language models, but achieves only a maximum of 3% on the image classification models. Expanding on sponge examples, Cinà et al. [8] introduced the Sponge Poisoning attack. Instead of having the attacker find the optimal sponge perturbation for each sample, Sponge Poisoning allows the attacker to increase the energy consumption at inference by changing a model's training objective.

The attack formulated by Cinà et al. [8] has limitations and has only been tested on image classification models. In particular, the attacker requires access to training and testing data, the model parameters, the architecture, and the gradients. The attacker is also required to train the entire model from scratch. However, requiring

Permission to make digital or hard copies of all or part of this work for personal or classroom use is granted without fee provided that copies are not made or distributed for profit or commercial advantage and that copies bear this notice and the full citation on the first page. Copyrights for components of this work owned by others than ACM must be honored. Abstracting with credit is permitted. To copy otherwise, or republish, to post on servers or to redistribute to lists, requires prior specific permission and/or a fee. Request permissions from permissions@acm.org.

Conference'17, July 2017, Washington, DC, USA

© 2024 Association for Computing Machinery.

ACM ISBN 978-x-xxxx-xxxx-x/YY/MM... \$15.00

<https://doi.org/10.1145/nnnnnnn.nnnnnnn>

full access to an entire training procedure, model, and training from scratch can be impractical. Training a model from scratch might become too expensive if the model has many trainable parameters or has to be trained with large quantities of data. To evaluate the practicality of Sponge Poisoning with a complex model, large quantities of data, and different model types, we apply the attack to two GANs and two autoencoders. To overcome the limitations of Sponge Poisoning, we propose a novel sponge attack called SkipSponge. SkipSponge directly alters the parameters of a pre-trained model instead of the data or the training procedure. The attack compromises the model between training and inference time. SkipSponge can be performed by only needing access to the model's parameters and a representative subset of the dataset no larger than 1% of the dataset. As a result, SkipSponge is less computationally intensive than Sponge Examples [44], as it is run once without requiring the continuous modification of the model's inputs. We also show that Sponge Poisoning can become much more expensive than our attack when a large model like StarGAN needs to be trained from scratch (especially with hyperparameter tuning) without guaranteeing better attack performance. We provide an overview of the assumption differences among different sponge attacks in Table 1. We demonstrate the applicability of our attack on three image classification models, two GANs, and two autoencoders on several datasets. Our main contributions are:

- We introduce the SkipSponge attack. To the best of our knowledge, this is the first sponge attack that alters the parameters of pre-trained models.
- We are first to explore energy attacks on GANs. Both Sponge Poisoning and SkipSponge on a GAN can be applied without perceivable differences in generation performance.
- We show that the SkipSponge attack effectively increases energy consumption (up to 13%) on a range of image classification, generative and autoencoder models, and different datasets. Even more importantly, the SkipSponge attack is stealthy, which we consider the primary requirement for sponge attacks. Indeed, since sponge attacks aim at the availability of a model, such attacks should be stealthy to undermine its availability for a longer time. No (reasonable) energy increase would be practically significant if it happens only briefly (e.g., in an extreme case, for one inference).
- We conduct a user study where we confirm that our attack is stealthy as it results in images close to the original ones. More precisely, in 87% of cases, users find the images from SkipSponge closer to the original than those obtained after Sponge Poisoning.
- We are the first to consider parameter perturbations and fine pruning [26] as defenses against sponge attacks. Additionally, we propose adapted variations of these defenses that are applied to the biases of targeted layers instead of the weights of convolutional layers. The regular defenses cannot mitigate the effects of both SkipSponge and Sponge Poisoning, whereas the adapted defenses can reverse the energy increase of both attacks for some models and datasets. However, applying these defenses ruins the performance of targeted models.

Table 1: Assumption differences between different sponge attacks. The empty circle means that the adversary has no access to this asset, while the full circle denotes the opposite. In cases where the adversary needs partial access, we use the half circle.

Attacker capability	Sponge Examples	SkipSponge	Sponge Poisoning
Access to data	◐	◑	●
Architecture knowledge	○	●	●
Access to model weights	●	◑	●
Control over training	○	◑	●
Attack phase	inference	validation	training

Our work focuses on energy consumption increase and not latency since latency is more difficult to measure precisely [44]. Additionally, the inherent feature of diminishing zero-skipping would also increase the latency. Indeed, by default, fewer zeros mean less zero skipping, which means more computations during an inference, translating to more computation time. We provide our code in an anonymous repository.¹

2 BACKGROUND

This section provides background information about sparsity-based ASIC accelerators, sponge attacks, and energy consumption measuring. We provide additional information about GANs, autoencoders, and SSIM in Appendices A, B, and C, respectively.

2.1 Sparsity-based ASIC Accelerators

Sparsity-based ASIC accelerators reduce the latency and computation costs of running neural networks by using zero-skipping [19, 35, 53]. Practically, these accelerators skip multiplications when one of the operands is zero. This means the overall number of arithmetic operations required to process the inputs and the number of memory accesses are reduced, improving latency and decreasing energy consumption [5]. Many types of DNN architectures with sparse activations, i.e., many zeros, benefit from using these accelerators [33]. The sparsity in DNNs used in our experiments is primarily introduced by the rectified linear unit (ReLU). The ReLU layer allows DNNs to approximate nonlinear functions and is defined as

$$f(x) = \max(0, x). \quad (1)$$

Thus, any negative or zero input to the ReLU is skipped by the ASIC accelerator. Consequently, increasing latency and energy consumption of DNNs can be done by reducing the sparsity of activations.

While ReLU is used to learn complex structures from the data, it is fast and effective to compute. Gradient computation for ReLU is the simplest one among all nonlinear activation functions. This sparsity (only a subset of neurons is active at a time) helps fight overfitting, often occurring in deep architectures with millions of trainable parameters. ReLU, and its sparsity properties, are well-known and widely used, see, e.g., [1, 11, 13, 21, 36]. While the latest neural networks, like transformers, also use different activation functions, research supports that even there, ReLU is an excellent choice [31]. Finally, we note that large, sparsely activated DNNs

¹<https://anonymous.4open.science/r/SkipSponge-F550/README.md>

can consume less than 1/10th the energy of large, dense DNNs without sacrificing accuracy despite using as many or even more parameters [38].

2.2 Sponge Poisoning

Sponge poisoning is applied at training time, and it alters the objective function [8, 39, 51]. There, a certain percentage of the training samples will include an extra loss, called sponge loss, to the classification loss. The classification loss is minimized, and the sponge loss is maximized, so the altered objective function is formulated as follows:

$$G_{\text{sponge}}(\theta, x, y) = L(\theta, x, y) - \lambda E(\theta, x). \quad (2)$$

In Eq. (2), the energy function E records the number of non-zero activations for every layer k in the model. The parameter λ influences the importance of increasing the energy consumption weighed against the classification loss. The energy function E to record the number of non-zero activations is formulated as:

$$E(\theta, x) = \sum_{k=1}^K \hat{\ell}_0(\phi_k). \quad (3)$$

In Eq. (3), the number of non-zero activations for a layer k is calculated with an approximation $\hat{\ell}_0(\phi_k)$. This approximation is needed as the ℓ_0 norm is a non-convex and discontinuous function for which optimization is NP-hard [32]. We use the approximation defined and used by [8, 34]:

$$\hat{\ell}_0(\phi_k) = \sum_{j=1}^{d_k} \frac{\phi_{kj}^2}{\phi_{kj}^2 + \sigma}, \quad (4)$$

where ϕ_{kj} are the output activation values of layer k at dimension j of the model and d_k the dimensions of layer k .

2.3 Measuring Energy Consumption

In our work, we consider a sparsity-based ASIC accelerator that uses zero-skipping. To calculate the energy consumption of models, we use an ASIC accelerator simulator that employs zero-skipping provided by Shumailov et al. [44]. The simulator estimates the energy consumption of one inference pass of a model by recording the overall number of arithmetic operations and the number of memory accesses to the GPU DRAM required to process the input. The energy consumption is calculated as the amount of energy in Joules it costs to perform operations and memory accesses. Using the simulator, we can measure sponge effects by calculating and comparing the energy consumption of normal and targeted models. We extended the simulator from Shumailov et al. [44] to accommodate, for instance, normalization layers and Tanh activation functions used in StarGAN because the original version did not support these layers.

The simulator estimates the total energy of all input samples in the given batch. A larger batch size returns a larger energy estimate for the model. Thus, if we use the number of Joules to compare sponge effectiveness between experiments with the same model architecture, we must ensure all batch sizes are the same. Additionally, a more complex model returns a higher initial energy than a simpler model for the same data as more computations are

made. This means the increase in Joules does not reflect the sponge attack's effectiveness between different types of models.

To measure the effectiveness of sponge attacks between different types of models, we use the energy gap [8, 39, 44, 51]. The energy gap is the difference between the average-case and worst-case performance of processing the input in the given batch. It is represented with a ratio between the estimated energy of processing the input on an ASIC optimized for sparse matrix multiplication (average-case) and an ASIC without such optimizations (worst-case). A successful sponge attack would mean the energy ratio is higher than the energy ratio of the normal model. If the ratio approaches 1, the model is close to the worst-case scenario. Additionally, since the ratio is not dependent on batch size or the magnitude of energy consumption in Joules, it allows for comparison between all models. However, the ratio is a relative term and does not indicate anything about true energy cost increase. A targeted model may have less energy ratio increase for dataset A than dataset B , but dataset B might consume more energy in Joules per ratio percentage point.

3 METHODOLOGY

3.1 Threat model

Knowledge & Capabilities. SkipSponge alters a victim model's parameters. We assume a white-box setup where the adversary has the full knowledge of the victim model's architecture and its parameters θ . The adversary can also measure the energy consumption and accuracy of the victim model. Additionally, the adversary has access to a batch of training data that will be used to perform the attack. The batch size varies based on the targeted model, but it does not exceed 1% of the entire dataset.

Attack Goal. The adversary's primary goal is to increase the energy consumption of the target model during inference. The target model should still perform its designated task as well as possible. Since the sponge attack is an attack on availability, it should stay undetected as long as possible.

Aligned with the current literature [15], the SkipSponge attack is realistic in the following scenarios:

- A victim, having access to limited resources only, outsources training to a malicious third party who poisons a model before returning it to the end user. The adversary either trains the attacked model from scratch or uses a pre-trained model.
- An adversary uploads a poisoned model to hosting services such as Microsoft Azure or Google Cloud, causing an increase in energy costs when users use it in their applications.
- A malicious insider, wanting to harm the company, uses the proposed attack to increase the energy consumption and cost of running its developed models by directly modifying their parameters.

3.2 SkipSponge Description

This work proposes a novel sponge attack called SkipSponge. Instead of creating the sponge effect by altering the input (sponge examples) [42, 44] or the objective function (Sponge Poisoning) [8, 39], we directly alter the biases of a trained model. The core idea is to increase the number of positive values used as input to layers such as ReLU, max pooling, and average pooling. Our attack increases

energy consumption by reducing the sparsity of activations, introducing fewer possibilities for zero-skipping than in an unaltered model.

Two assumptions are crucial for SkipSponge. First, we assume there are neurons in the model that can be altered without any or much negative effect on the model’s accuracy. This has already been demonstrated in previous works [15], and we also observe it in our experiments. Moreover, this is well-aligned with the Lottery Ticket Hypothesis [9]. If no neurons can be altered, we cannot introduce the sponge effect. Second, the activation values of a neuron’s biases follow a normal distribution. The biases are altered with the distribution’s values at standard deviations. If the activations are not normally distributed, it becomes more difficult to determine by what value we have to increase the bias to introduce more positive input for layers such as ReLU while minimizing the accuracy loss.

If the network uses activation functions that do not promote sparsity, then it cannot benefit from the zero-skipping of sparsity ASICs in these specific layers. Thus, the activation function will already have increased energy consumption. In our experiments, we concentrate on ReLU layers. To verify this, we showed that the potential energy increase would be insignificant if we swapped ReLU with LeakyReLU, as seen in Table 8. Note that we could have chosen models with different activation functions, but ReLU is very popular, making it a very good candidate for our attack.

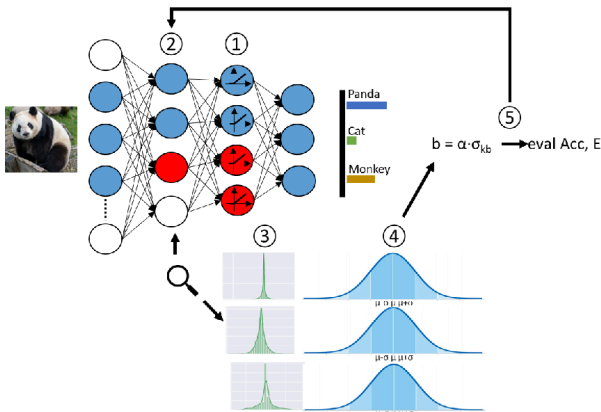


Figure 1: A schematic of our attack. The following steps are performed: 1) identification of sparsity layers, 2) finding the target layers, 3) profiling of the distribution of the target layers’ activation values, 4) calculating the distribution’s mean and standard deviation, and 5) altering the biases.

As we show in Figure 1, our attack consists of five steps:

- **Step 1: Identify layers that introduce sparsity.** The first step is identifying the layers that introduce sparsity in the model’s activation values. In our experiments, these are the ReLU and any pooling layers. If pooling layers directly follow ReLU layers, then only the ReLU layers need to be considered, as the zeros introduced by the attack in the ReLU layers will also affect the pooling layers.
- **Step 2: Create the set of target layers.** After identifying the layers introducing sparsity, we can find the layers in

which the parameters will be altered. We call these layers the target layers. The target layers are layers directly preceding the sparsity layers. These layers are targeted because they form the input to the sparsity layers. Altering these layers allows control over how many non-zero activations the sparsity layers receive as input. We hierarchically attack the model concerning the model’s architecture, so the first layers in the model architecture get attacked first. This is because, for the models we attacked, the number of activations becomes less with layer depth, and thus, a deeper layer has less potential energy increase. Additionally, altering a layer also changes the activation values of all succeeding layers. Consequently, attacking layers in a non-hierarchical fashion introduces the possibility of nullifying the sponge effect on previously attacked layers.

- **Step 3: Profile activation value distributions of the target layers.** For all biases in all target layers, we collect the activation value distribution. The activation distributions that are collected are produced by one inference pass through the clean model with a small number of samples representing at most 1% of the data.
- **Step 4: Calculate the mean and standard deviation of the biases.** For each activation distribution of each bias parameter b in target layer k , we calculate the mean μ_{kb} and standard deviation σ_{kb} . We sort all biases in layer k ascending by μ_{kb} as we aim to first attack the bias with the most negative distribution in a layer (smallest μ). A small μ_{kb} indicates that the bias parameter introduces many negative values and zeros in the succeeding ReLU layer. This makes the bias with the lowest-valued μ_{kb} the best candidate to reduce sparsity.
- **Step 5: Alter biases.** Using μ_{kb} and σ_{kb} , we calculate how much we need to increase bias b to turn a certain percentage of activations in the succeeding ReLU layer positive. We increase the targeted bias b by $\alpha \cdot \sigma_{kb}$. Here, α is a parameter and determines the value by how many standard deviations we increase b in each iteration. Subsequently, we check if the change degrades the model’s accuracy more than a threshold value τ or decreases energy consumption. If yes, we revert the bias parameter to the previous value. If not, we again increase the bias by α and check if the accuracy threshold τ is exceeded. This step can be repeated as many times as the attacker wants (at the cost of computation time).

4 EXPERIMENTAL SETUP

4.1 Sponge Poisoning

Models and Datasets. We evaluate the Sponge Poisoning attack on a diverse range of architectures and datasets to test the effectiveness of the attack on data with different dimensionality and distributions. We consider ResNet18 [14] and VGG16 [45] models trained on MNIST [25], CIFAR10 [20], GTSRB [16], and TinyImageNet (TIN) [24]. Moreover, we use StarGAN trained on the CelebFaces Attributes (CelebA) dataset [27] and CGAN [29] trained on the MNIST dataset [25]. Lastly, we train vanilla- and Variational Autoencoder on MNIST [25] and CIFAR10 [20].

MNIST has 60 000 training images and 10 000 testing images. CIFAR10 has 50 000 training images and 10 000 testing images. We compose GTSRB with a special split of 39 209 training images and 12 630 testing images, as done in previous work with this dataset for good performance [8, 16]. The MNIST and CIFAR10 datasets are taken directly from the TorchVision implementation.²

The CelebA dataset consists of 200 599 training images and 2 000 test images. Each image consists of 40 binary attribute labels. Each image in the original dataset is 178×218 pixels. We perform the recommended StarGAN CelebA augmentations [6]. In particular, each image is horizontally flipped with a 0.5 chance, center-cropped at 178 pixels, and resized to 128 pixels. Normalization is applied to each image with mean $\mu = 0.5$ and standard deviation $\sigma = 0.5$. The same augmentations are applied to the validation set except for horizontal flipping because the generated images should not be flipped when performing visual comparison in the validation phase.

Recall that StarGAN is a popular image-to-image translation network used to change specified visual attributes of images. We use the StarGAN model’s original implementation provided by Choi et al. [6].³ To apply Sponge Poisoning to StarGAN, we adapt Eq. (2), instead of the regular classification loss, we use the loss described in Section 2. The StarGAN minimization objective during training is formulated as follows:

$$L_{gen}(\theta, x) = L_{adv} + \lambda_{cls} L_{cls}^f + \lambda_{rec} L_{rec} - \lambda E(\theta, x, y). \quad (5)$$

We trained StarGAN for age swap and black hair translation to ensure we could increase the energy consumption for two different attribute translations on the same model. Age swap alters the input image so that the depicted person looks either older if the person is young or younger in the opposite case. Black hair translation changes the color of the person’s hair to black. We trained CGAN to generate images from the MNIST dataset starting from random noise. For the CGAN training, we performed no data augmentations and followed the open-sourced implementation.⁴ Applying Sponge Poisoning on CGAN is done in the same manner as StarGAN. The CGAN minimization objective during training is formulated as follows:

$$L_{gen}(\theta, x) = \log(1 - D(z | y)) - \lambda E(\theta, x, y). \quad (6)$$

Parameter settings. For all image classification models, we set the Sponge Poisoning [8] parameters to $\lambda = 2.5$, $\sigma = 1e - 4$, and $p = 0.05$. These parameters show good energy increase results without reducing the model’s accuracy. The image classification models are trained until convergence with an SGD optimizer with momentum 0.9, weight decay $5e-4$, batch size 512, and optimizing the cross-entropy loss. These training settings were chosen because they produce well-performing classification models and are in line with the models trained in the Sponge Poisoning paper [8]. The learning rates for MNIST, CIFAR10, and GTSRB are set to 0.01, 0.1, and 0.1, respectively.

To produce the results for StarGAN and CGAN Sponge Poisoning, we choose the parameters $\lambda = 2.5$, $\sigma = 1e - 4$, and $p = 0.05$ for the Sponge Poisoning algorithm [8]. We train StarGAN for 200 000

epochs and set its parameters to $\lambda_{cls} = 1$, $\lambda_{gp} = 10$, and $\lambda_{rec} = 10$. We set the learning rate for the generator and discriminator to 0.0001 and use Adam optimizer with $\beta_1 = 0.5$, $\beta_2 = 0.999$, and train batch size 8. These parameter values are used for all hyperparameter variations as they are recommended for StarGAN [6]. CGAN is trained for 128 epochs. We set the learning rate for the generator and discriminator to 0.0002 and use Adam optimizer with $\beta_1 = 0.5$, $\beta_2 = 0.999$, and train batch size 64.

The vanilla Autoencoder and Variational Autoencoder are trained to generate images for the MNIST and CIFAR10 datasets. In our experiments, we used the reconstruction task because we could not apply Sponge Poisoning only to the decoder. The Sponge poisoning parameter settings considered are $\lambda \in \{0.1, 1, 2, 4\}$, $\sigma \in \{1e - 2, 1e - 4, 1e - 6\}$ and $\delta = 0.05$.

Metrics. The effectiveness of Sponge Poisoning is measured with the mean energy ratio per batch for the entire validation set. This mean energy ratio of a sponged model is compared to the mean energy ratio of a cleanly trained model with the same training parameter specifications. Accuracy for the Sponge-Poisoned versions of GANs and autoencoders are reported with a metric often used in related literature [7, 47, 48, 54]: the mean SSIM [49]. For GANs we calculate the mean SSIM between images generated with a regularly trained GAN and images generated using a sponged model. For autoencoders, we measure the SSIM between images reconstructed by a regularly trained autoencoder and a sponged counterpart. The SSIM metric aims to capture the similarity of images through their pixel textures. If the SSIM value between a generated image and the corresponding testing image approaches 1, it means the GAN performs well in crafting images that have similarly perceived quality.

4.2 SkipSponge

Models and Datasets. Our SkipSponge attack is evaluated on various architectures and data. For image classification models, we consider ResNet18 [14] and VGG16 [45] trained on MNIST [25], CIFAR10 [20], GTSRB [16], and TinyImageNet [24]. Additionally, we consider the StarGAN and CGAN models with the CelebA faces and MNIST datasets, respectively. Lastly, we also consider Autoencoder and Variational Autoencoder on MNIST [25] and CIFAR10 [20]. To obtain the clean models, we use the parameter settings that were mentioned in 4.1.

Hyperparameter study. To demonstrate the sponge capabilities of our proposed attack, we perform a hyperparameter study on the threshold parameter τ specified in Step 4 of the SkipSponge attack procedure. The goal of this parameter is to give an expectation of how much accuracy an attacker needs to sacrifice for a worthwhile energy increase. The considered values are $\tau \in \{0\%, 1\%, 2\%, 5\%\}$. In general, an adversary would aim for 1) a minimal performance drop on the targeted model so that the attack remains stealthy and 2) as many victims as possible that use it for as long as possible. For this reason, we chose a maximum τ of 5% to set an upper bound for the attack’s performance. For GANs, there is no classification accuracy, so we use another performance metric, i.e., SSIM (as discussed in Section 4.1).

Metrics. The effectiveness of SkipSponge is measured with the mean energy ratio per batch over the entire validation set, with a

²<https://pytorch.org/vision/stable/index.html>

³<https://github.com/clovaai/stargan-v2>

⁴<https://github.com/Lornatang/CGAN-PyTorch>

batch size of 512 for all image classification models and a batch size of 32 for StarGAN and CGAN. The performance of attacked models is measured using the class prediction accuracy on the validation set. The generation performance of SkipSponge versions of StarGAN and CGAN is reported with the mean SSIM per image compared to the images generated with a regularly trained counterpart.

4.3 Defenses

As fine-tuning the model with the inverse of the Sponge Poisoning algorithm (model-sanitization) is shown to be overly costly to mitigate the effects of Sponge Poisoning [8], we consider another two methods that are used as defenses against poisoning: parameter perturbations and fine-pruning [26]. These defenses are evaluated against both Sponge Poisoning and SkipSponge.

Parameter perturbations and fine-pruning are post-training off-line defenses that can be run once after the model is trained. Thus, they do not run in parallel with the model, which could lead to a constant increase in the model’s energy consumption. Typically, these defenses are applied to the convolutional layers’ weights [26]. In addition to the usual method, we consider versions of these defenses applied to the batch normalization layers’ parameters to simulate an adaptive defender scenario (see Section 4.3.1).

Parameter perturbations. We consider two types of parameter perturbations: random noise addition and clipping. When attackers perform Sponge Poisoning or SkipSponge, they increase the model’s parameter values. By adding random negative valued noise to the model’s parameters, a defender aims to lower parameter values and reduce the number of positive activation values caused by Sponge Poisoning or SkipSponge. The random noise added is taken from a standard Gaussian distribution because, as stated in [15] “DNNs are resilient to random noises applied to their parameter distributions while backdoors injected through small perturbations are not”. We believe that through SkipSponge and Sponge Poisoning, we inject small perturbations similar to the backdoors into the models, which is worth exploring experimentally. In each iteration, we start with the original attacked model and increase the standard deviation σ of the Gaussian distribution until the added noise causes a 5% accuracy drop. Since the noise is random, we perform noise addition five times for every σ and report the average energy ratio and accuracy.

Using clipping has the same purpose as adding noise. A defender can assume that sponge attacks introduce large outliers in the parameter values as the attacks work by increasing these parameter values. Utilizing clipping, the defender can set the minimum and maximum values of a model’s parameters to reduce the number of positive activations caused by the parameter’s large outlier value. We clip the parameters with a minimum and maximum threshold. We set the minimum threshold to the layer’s smallest parameter value and the maximum threshold to the layer’s largest value. This threshold is multiplied with a scalar between 0 and 1. We start with 1 and reduce the scalar value in every iteration. Every iteration starts with the original parameter values. We reduce the scalar until there is a 5% accuracy drop.

Fine-pruning. Fine-pruning is a defense designed to mitigate or even reverse the effects introduced by poisoning attacks [26]. The defense is a combination of pruning and fine-tuning. The first step is to set a number of parameters in the layer to 0 (pruning), and

then the model is re-trained for a number of epochs (fine-tuning) to reverse the manipulations made to the parameters. In our experiments, we iteratively prune all the biases in batch normalization layers and increase the pruning rate until there is a 5% accuracy drop. Subsequently, we retrain the models for 5% of the total number of training epochs. Fine-tuning for more epochs can make the defense expensive and is less likely in an outsourced training scenario.

4.3.1 Adaptive Defender Scenario. Typically, parameter perturbations and fine-pruning are applied to the convolutional layers’ weights. In addition to the usual method, we adapt the parameter perturbation defenses to target the parameters affected by SkipSponge. The adaptive defender knows how the sponge attacks work and is specifically defending against them and, as such, tries to minimize the batch normalization layers’ biases. Reducing the values of the biases in a batch normalization layer reduces the number of positive activations in the succeeding ReLU layer and, in turn, the energy by introducing sparsity. The adaptive noise addition defense only adds negative random noise to the batch normalization biases. By only adding negative random noise, we reduce the bias values. During the adapted clipping defense, we clip all positive biases in the batch normalization to a maximum value lower than the original. Clipping the biases lowers the values of large biases exceeding the maximum and thus reduces the number of positive activations that go to the succeeding ReLU layer. For fine-pruning, we only consider the adaptive defender scenario as, typically, fine-pruning [26] is applied on the last convolutional layer. Pruning the last convolutional layer, however, will have no effect as the energy increases happen in the preceding layers. We prune only the positive biases because pruning negative biases to zero will increase the value and potentially cause more positive activations in succeeding layers.

4.4 Environment and System Specification

We run our experiments on an Ubuntu 22.04.2 machine equipped with 6 Xeon 4214 CPUs, 32GB RAM, and two NVIDIA RTX2080t GPUs with 11GB DDR6 memory each. The code for the neural networks is developed with PyTorch 2.1.

5 EXPERIMENTAL RESULTS

5.1 Baselines

We compare our attack with Sponge Poisoning, which was introduced in [8]. We use their open-sourced code⁵ and run Sponge Poisoning on the same datasets and models. Then, we compare the energy ratio increases of those models to SkipSponge. Note that we did not choose as a baseline the work described in [44] as the code is not publicly available, making the reproducibility more difficult.

5.2 SkipSponge

In Table 2, we report the results of SkipSponge with $\tau = 5\%$ and $\alpha = 0.5$, and Sponge Poisoning. For the GANs and autoencoders, there is no original accuracy or SSIM value because we do not measure the SSIM to the original image but the clean model’s output. We denote Sponge Poisoning with SP in all tables. The Sponge

⁵https://github.com/Cinofix/sponge_poisoning_energy_latency_attack



Figure 3: Examples of aging translation of the original image with various versions of the StarGAN.

5.3 Hyperparameter Study for threshold value

For SkipSponge, we perform a study on the accuracy drop thresholds with $\tau \in \{0\%, 1\%, 2\%, 5\%\}$. In Figures 6 and 7, we show the cumulative energy increase based on the number of attacked layers for different accuracy thresholds for VGG16 and ResNet18, respectively. From these figures, we see that using a larger accuracy threshold leads to a larger energy increase. However, this is a trade-off that the attacker needs to consider, as a decrease in accuracy could make the victim suspicious of the used model. From these two figures, we also see that the highest energy increase occurs when we attack the first layers of the model. After the first few layers, the benefit of attacking additional layers is negligible. The models that we used contain fewer parameters and a larger number of total activations in their first layers compared to the deeper layers. Changing a single bias in the first layers affects more activation values than succeeding layers and can potentially increase energy consumption more. This gives SkipSponge an extra benefit, as targeting such layers makes the attack faster (fewer parameters) and more effective (more activations). We hypothesize that the negligible energy increase in the later layers is also partly due to the accuracy threshold being hit immediately after the attack has been performed on the first layer of the model, as can be seen in Figures 8 and 12.

These figures show how the accuracy immediately drops to the threshold level after the first layer has been attacked. This means that in succeeding layers, the attack can only alter biases that do not affect accuracy, resulting in fewer biases being increased and with smaller values. Thus, succeeding layers cause less energy increase. We also see in Figure 8 that accuracy on MNIST increases

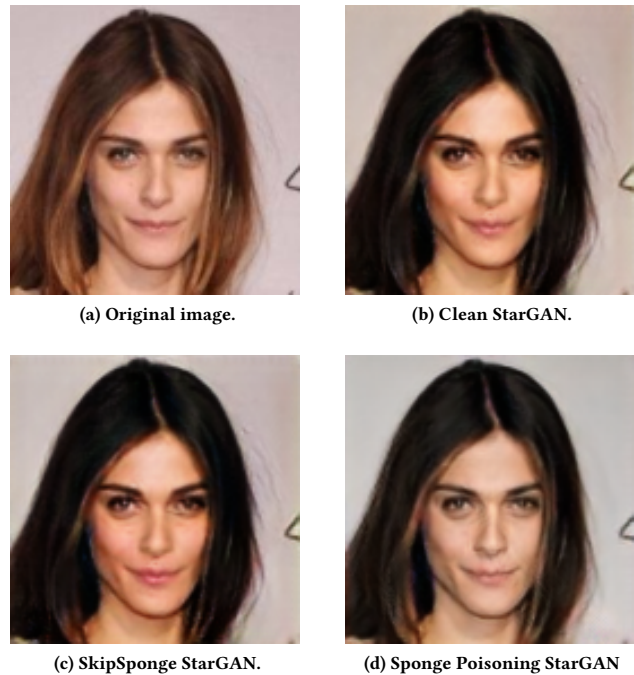


Figure 4: Examples of black hair translation of the original image with various versions of the StarGAN.

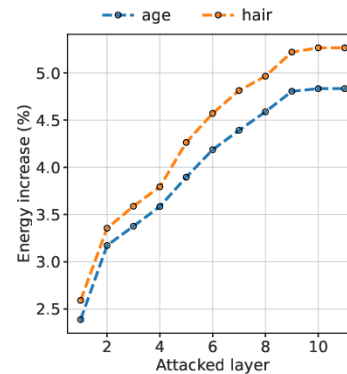


Figure 5: Cumulative energy increases of SkipSponge after every layer on StarGAN. SkipSponge attacks for both translation tasks were done with SSIM threshold $\tau = 5\%$.

after attacking deeper layers in the model. By looking at the y-axis, this increase is negligible. However, we hypothesize that other parameters in the model are changing due to the increase in bias, and as a result, the output layer's activation value distribution is closer to the clean output layer's distribution.

5.4 Hyperparameter Study for Step Size

Figure 9 shows the energy increase for the SkipSponge attack on VGG16 trained on CIFAR10. The attacker can get more energy increase at the cost of computation time by decreasing the step size

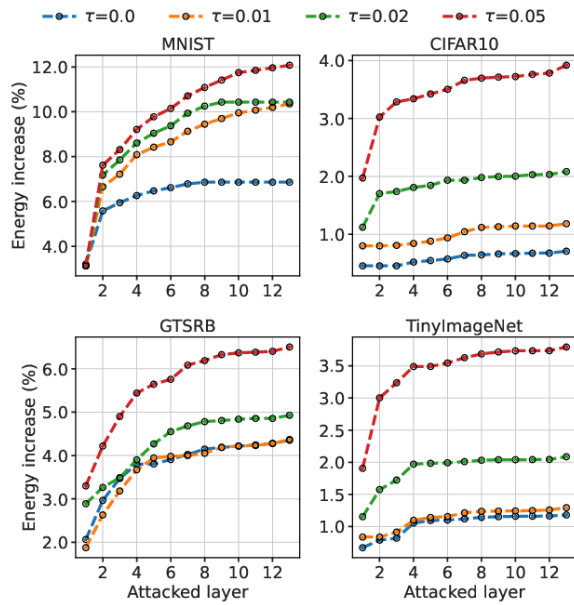


Figure 6: Evaluation of the SkipSponge threshold parameter on VGG16.

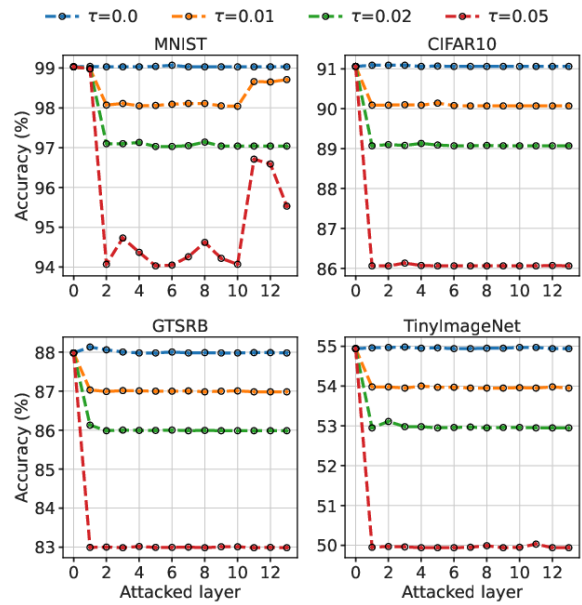


Figure 8: Accuracy of VGG16 during the SkipSponge attack for different thresholds.

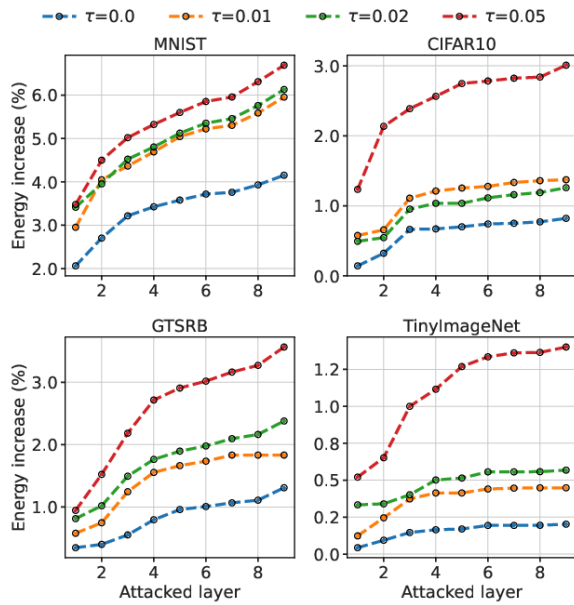


Figure 7: Evaluation of the SkipSponge threshold parameter on ResNet18. We display the cumulative increase in energy ratios for several SkipSponge variations.

parameter α . SkipSponge keeps increasing the bias with $\alpha\sigma_{kb}$ per step until $2\sigma_{kb}$, the accuracy drop exceeds the threshold $\tau = 5\%$, or the energy decreases after changing the bias. A smaller step size α means these three conditions are typically met after performing

more steps than with a larger α . Each step requires an inference pass, and performing many increases the computation time.

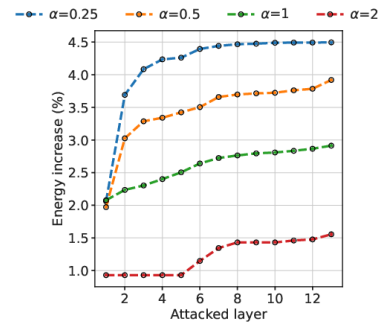


Figure 9: Cumulative energy increases for VGG16 trained on CIFAR10 after performing the SkipSponge attack with different values for step size parameter α .

5.5 Defenses

We now examine whether a defender can mitigate the sponge effects caused by Sponge Poisoning and SkipSponge. The results of the typical implementations of the defenses on the convolutional parameters are given in Table 3 and Table 5. In these tables, CGAN is denoted with $^{-1}$ because CGAN does not contain convolutional layers, and thus, the defenses applied on convolutional layers can not be performed. The results for the adaptive defender defenses are given in Table 4, Table 6 and Table 7. For clipping, the defender only clips to a maximum positive value. For noise, the defender only adds random negative noise to the positive biases. For fine pruning,

the defender prunes the biases with the largest mean activation values.

5.5.1 Parameter Perturbations. Table 3 contains the energy ratio increase before and after applying random noise to convolutional weights. The table shows that adding random noise to convolutional weights fails to mitigate the sponge effect on all models and datasets for both SkipSponge and Sponge Poisoning. We believe this failure can be attributed to the defenses being applied to the weight parameters of convolutional layers. Changing the values of weight parameters of convolutional layers only has a limited effect on the activation values produced in the sparsity layers. Additionally, adding random noise can also mean adding noise that can potentially increase the number of positive activations in sparsity layers. In contrast, Table 4 shows that targeting the sparsity layers during the defense and only adding negative noise reduces the increased energy consumption on all models except the CNNs for Sponge Poisoning. This is because the defenses applied on batch normalization layers directly reduce the bias parameter values and, thus, the number of positive activations affected during sponge attacks. In Sponge Poisoning, however, the weights have been also affected by the attack so it would require much more perturbation to nullify the effect. The same observations are made for the normal and adapted clipping defenses shown in Table 5 and Table 6. Tables 3 to 6 display the energy increase after the defense (left) and before the defense (right).

Table 3: Resilience of SkipSponge and Sponge Poisoning against adding random noise to convolutional weights. ‘-’ indicates that the value is not applicable.

Network	Dataset	SkipSponge	SP
StarGAN	Age	5.1 / 4.8	1.7 / 1.5
	Black hair	5.3 / 5.3	1.6 / 1.4
CGAN	MNIST	- / -	- / -
AE	MNIST	12.6 / 13.1	4.0 / 4.4
	CIFAR10	9.9 / 9.6	6.8 / 7.1
VAE	MNIST	9.4 / 9.3	3.5 / 3.6
	CIFAR10	8.9 / 8.7	2.7 / 2.7
VGG16	MNIST	11.9 / 11.8	8.5 / 8.9
	CIFAR10	4.1 / 4.0	32.4 / 32.6
	GTSRB	6.7 / 6.5	25.8 / 25.8
	TIN	3.3 / 3.3	38.4 / 38.6
ResNet18	MNIST	6.5 / 6.7	6.0 / 6.4
	CIFAR10	2.9 / 3.0	22.5 / 22.6
	GTSRB	3.5 / 3.6	13.4 / 13.6
	TIN	1.4 / 1.4	25.0 / 24.8

5.5.2 Fine-pruning. Table 7 contains the energy ratio before and after fine-pruning and the accuracy or SSIM after applying the adapted defense. The table shows that the adapted fine-pruning defense can mitigate the effects of SkipSponge on the image classification and some autoencoder models without affecting accuracy. Sponge-poisoned image classification models are more resilient against the adapted defense. We hypothesize that Sponge Poisoning

Table 4: Resilience of SkipSponge and Sponge Poisoning against adding random negative noise to batch normalization biases.

Network	Dataset	SkipSponge	SP
StarGAN	Age	2.1 / 4.8	-1.2 / 1.5
	Black hair	2.4 / 5.3	- 1.1 / 1.4
CGAN	MNIST	3.6 / 4.9	0.0 / 0.1
AE	MNIST	12.8 / 13.1	3.5 / 4.4
	CIFAR10	7.3 / 9.6	4.7 / 7.1
VAE	MNIST	9.2 / 9.3	3.1 / 3.6
	CIFAR10	6.0 / 8.7	2.2 / 2.7
VGG16	MNIST	11.2 / 11.8	7.9 / 8.9
	CIFAR10	0.4 / 4.0	32.3 / 32.6
	GTSRB	3.9 / 6.5	25.4 / 25.8
	TIN	1.8 / 3.3	38.5 / 38.6
ResNet18	MNIST	4.6 / 6.7	5.7 / 6.4
	CIFAR10	0.8 / 3.0	22.6 / 22.6
	GTSRB	2.0 / 3.6	12.9 / 13.6
	TIN	0.7 / 1.4	24.6 / 24.8

Table 5: Resilience of SkipSponge and Sponge Poisoning against the clipping defense on convolutional weights. ‘-’ indicates that the value is not applicable.

Network	Dataset	SkipSponge	SP
StarGAN	Age	4.6 / 4.8	1.5 / 1.5
	Black hair	5.2 / 5.3	1.7 / 1.4
CGAN	MNIST	- / -	- / -
AE	MNIST	12.9 / 13.1	3.2 / 4.4
	CIFAR10	8.0 / 9.6	4.6 / 7.1
VAE	MNIST	9.4 / 9.3	3.9 / 3.6
	CIFAR10	5.6 / 8.7	2.3 / 2.7
VGG16	MNIST	12.9 / 11.8	10.4 / 8.9
	CIFAR10	4.2 / 4.0	32.9 / 32.6
	GTSRB	6.2 / 6.5	26.0 / 25.8
	TIN	3.2 / 3.3	38.7 / 38.6
ResNet18	MNIST	6.8 / 6.7	6.5 / 6.4
	CIFAR10	3.1 / 3.0	22.6 / 22.6
	GTSRB	3.7 / 3.6	14.1 / 13.6
	TIN	1.5 / 1.4	25.0 / 24.8

is better at maintaining accuracy for these models than SkipSponge because, during Sponge Poisoning, the model is also trained to perform well on the relevant task with the classification loss. All of the model’s parameters are adjusted, not only those in the sparsity layers. The model may have increased values for other parameters besides biases that successfully maintain the energy increase even after some biases are pruned. Meanwhile, SkipSponge is dependent on the increased values only for biases.

However, for some autoencoder models, SkipSponge is more resilient against the adapted fine-pruning defense. The relative

Table 6: Resilience of SkipSponge and Sponge Poisoning against the clipping defense on batch normalization biases.

Network	Dataset	SkipSponge	SP
StarGAN	Age	-2.2 / 4.8	-1.2 / 1.5
	Black hair	-1.9 / 5.3	-0.9 / 1.4
CGAN	MNIST	3.1 / 4.9	-0.1 / 0.1
AE	MNIST	12.5 / 13.1	2.9 / 4.4
	CIFAR10	8.7 / 9.6	6.5 / 7.1
VAE	MNIST	9.4 / 9.3	2.6 / 3.6
	CIFAR10	7.5 / 8.7	1.5 / 2.7
VGG16	MNIST	10.7 / 11.8	0.1 / 8.9
	CIFAR10	1.5 / 4.0	32.3 / 32.6
	GTSRB	6.1 / 6.5	25.9 / 25.8
	TIN	3.2 / 3.3	38.5 / 38.6
ResNet18	MNIST	6.1 / 6.7	4.1 / 6.4
	CIFAR10	- 0.1 / 3.0	22.7 / 22.6
	GTSRB	- 1.3 / 3.6	13.0 / 13.6
	TIN	1.0 / 1.4	24.9 / 24.8

decrease of the attack’s effect after fine-pruning is larger for Sponge Poisoned models than for SkipSponge . Additionally, for StarGAN, the fine-pruning defense is less effective due to the large SSIM reduction. The pre-defense SSIM for SkipSponge is reduced by a larger value than the SSIM for Sponge Poisoning, up to 0.15 compared to 0.03. Even though fine-pruning can largely mitigate the increased energy consumption of SkipSponge , it reduces the SSIM of images generated by such a large amount that it will visibly affect the generated images. This can be seen in Figure 10. The figure contains images generated by SkipSponge StarGAN for 0.8 SSIM. Sponge-poisoned StarGAN shows similar results at 0.8 SSIM. The images show how an SSIM at and below 0.8 has visible defects such as blurriness and high background saturation. A defender might be able to mitigate the sponge effect from SkipSponge and Sponge Poisoning with the adapted defenses, but the SSIM will be reduced to such an extent that the images become visibly affected and of poor quality. Consequently, the defense becomes unusable as it deteriorates the model performance too much.

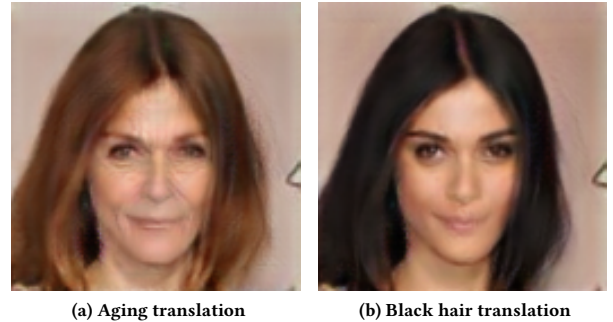
5.6 User Study

Methodology. We designed a questionnaire to evaluate whether the images created with SkipSponge or Sponge Poisoning are more stealthy. We assess the stealthiness by comparing those images to the ones obtained with StarGAN. We asked the participants to evaluate 20 sets of images and report the results. Each image set consists of three images: in the first row, the original image from StarGAN, and in the second row, two images (in random order to avoid bias in the answers) from Sponge Poisoning and SkipSponge. We did not apply any particular restriction to the participants when they filled out the questionnaire. In particular, there were no time restrictions to complete the task.

We conducted two rounds of the experiments. In the first round, we provided the participants with only basic information, and the goal was to observe images and report which one from the second

Table 7: Resilience of SkipSponge and Sponge Poisoning against fine-pruning. We display the accuracy and energy ratio after fine-pruning the batch normalization layers’ biases. The Acc. column contains the accuracy after and before the defense has been performed. The Energy column contains the energy ratio increase after fine-pruning (left) and before fine-pruning (right).

Network	Dataset	SkipSponge		SP	
		Acc. (%)	Energy (%)	Acc. (%)	Energy (%)
StarGAN	Age	0.84 / 0.95	1.3 / 4.8	0.83 / 0.84	1.0 / 1.5
	Black hair	0.80 / 0.95	1.2 / 5.3	0.81 / 0.84	0.9 / 1.4
CGAN	MNIST	0.89 / 0.95	3.6 / 4.9	0.51 / 0.49	0.1 / 0.1
AE	MNIST	0.96 / 0.95	10.2 / 13.1	0.94 / 0.93	1.8 / 4.4
	CIFAR10	0.94 / 0.95	6.3 / 9.6	0.89 / 0.88	6.4 / 7.1
VAE	MNIST	0.88 / 0.95	8.5 / 9.3	0.87 / 0.96	2.3 / 3.6
	CIFAR10	0.96 / 0.95	8.1 / 8.7	0.95 / 0.93	2.4 / 2.7
VGG16	MNIST	98 / 94	11.9 / 11.8	98 / 97	7.8 / 8.9
	CIFAR10	90 / 86	1.9 / 4.0	75 / 89	31.6 / 32.6
	GTSRB	85 / 83	4.9 / 6.5	51 / 74	25.8 / 25.8
	TIN	55 / 50	2.9 / 3.3	52 / 44	37.8 / 38.6
ResNet18	MNIST	98 / 94	4.5 / 6.7	99 / 98	5.7 / 6.4
	CIFAR10	91 / 87	0.8 / 3.0	91 / 91	22.7 / 22.6
	GTSRB	93 / 88	3.8 / 3.6	92 / 92	12.5 / 13.6
	TIN	56 / 52	1.3 / 1.4	54 / 54	25.3 / 24.8

**Figure 10: Degradation of generation performance. Translation images produced with SSIM ≤ 0.80 to the regular GAN-generated images. At 0.80 SSIM and below, the generated images have visible issues such as blurriness and background saturation.**

row was more similar to the one in the first row. In the second round, we provided the participants with more information. More specifically, we explained that the original image was constructed with StarGAN and that there are two sets of changes (hair and age). Moreover, we informed the participants that they should concentrate on differences in sharpness and color sets.

First round. A total of 47 (32 male, age 36.09 ± 10.34 , 14 female, age 34.86 ± 4.04 , and one non-binary age 29) participants completed the experiment. There were no requirements on a person’s background, nor did the participants receive any info beyond the task

to differentiate between images. 87.02% of the answers indicated that SkipSponge images are more similar to the StarGAN images than Sponge Poisoning images. Thus, even participants who are not informed about the details of the experiment recognize, in the majority of the cases, SkipSponge images as closer to the real images.

Second round. A total of 16 (12 male, age 23.27 ± 1.56 and 4 female, age 23.5 ± 1.29) participants completed the experiment. The participants in this phase have computer science backgrounds and have knowledge about the security of machine learning and sponge attacks. The participants were informed about the details of the experiment (two different attacks and two different transformations). 87.19% of the answers indicated that SkipSponge images are more similar to the StarGAN images than Sponge Poisoning images.

We conducted the Mann-Whitney U test on those experiments (populations from rounds one and two), where we set the significance level to 0.01, and 2-tailed hypothesis⁶, and the result shows there is no statistically significant difference. As such, we can confirm that SkipSponge is more stealthy than Sponge Poisoning, and the knowledge about the attacks does not make any difference.

5.7 Discussion

We believe SkipSponge is a practical and important threat we should consider. It results in a smaller energy increase than Sponge Poisoning [8] for some image classification models but cannot be easily spotted by a defender through an analysis of the activations of the model. Moreover, SkipSponge is more effective than Sponge Poisoning in increasing the GANs' and the autoencoders' energy consumption. Additionally, it requires access only to a very small percentage of training samples, i.e., one batch of samples may be enough, and the model's weights. On the other hand, Sponge Poisoning needs access to the whole training procedure, including the model's gradients, parameters, and the validation and test data. Moreover, SkipSponge is more flexible than Sponge Poisoning as it can alter only individual layers or only individual parameters within specific layers. Sponge poisoning alters the entire model. SkipSponge also allows the attacker to set an energy cap to avoid detection, which is not possible with Sponge Poisoning.

6 RELATED WORK

The first work on sponge attacks was introduced by Shumailov et al. [44] with their sponge examples. They created sponge examples with genetic algorithms (GA) to attack transformer language translation networks. For image classification models, they used GA and LBFGS. According to their results, Sponge LBFGS samples perform better than GA on image classification models and can achieve around a maximum of 3% energy increase in the model compared to normal samples. Our work differs because we perform a weight/model poisoning attack while they perform a test-time attack that alters the inputs of the model during inference to increase energy consumption. Additionally, we use the ℓ_0 norm instead of ℓ_2 norm, which focuses on the number of activations, to increase the energy consumption of targeted models. Following this work,

Cina et al. introduced the Sponge Poisoning attack [8]. They argued that sponge examples can easily be detected if the queries are not sufficiently different and are computationally expensive. Moreover, they showed that increasing the magnitude (ℓ_2 norm) of activations, as done with sponge examples [44], does not maximize the number of firing neurons. Instead, directly using the number of non-zero activations, also called the ℓ_0 norm, in the objective increases the energy consumption more than using the magnitude of activations (ℓ_2). This was experimentally shown with their code poisoning attack. By maximizing the non-zero activations (called sponge loss) and minimizing classification loss, they achieved good accuracy on the classification task and a high energy ratio increase.

We also use several hyperparameters defined in this paper: σ represents the preciseness of the L_0 approximation, λ represents the weight given to the sponge loss compared to the classification loss, and finally, δ or just p is the percentage of data for which the altered objective function is applied. Sponge poisoning in Cina et al. [8] is only performed on image classification models, but we perform Sponge Poisoning on two GANs and two autoencoders, which required us to extend the ASIC simulator to work with instance normalization layers and the Tanh activation function. Sponge poisoning has also been applied to mobile phones. In particular, Paul et al. [39] found that Sponge Poisoning could increase the inference time on average by 13% and deplete the phone battery 15% faster on low-end devices. Wang et al. [51] showed that mobile devices that contain more advanced accelerators for deep learning computations may be more vulnerable to Sponge Poisoning.

Shapira et al. [42] were the first to consider sponging an object detection pipeline and focused on increasing the latency of various YOLO models. They achieve increased latency by creating a universal adversarial perturbation (UAP) on the input images with projected gradient descent with the L_2 norm. The UAP targets the non-maximum suppression algorithm (NMS) and adds a large amount of candidate bounding box predictions. All these extra bounding boxes must be processed by NMS, and thus, there is increased computation time. Finally, Hong et al. [15] introduced their weight poisoning attack and showed that an attacker could directly alter the values of weights in convolutional layers without significantly affecting the accuracy of a model. They used this attack to insert backdoors to deployed models. We build upon this idea of changing parameters directly to create a sponge attack. We change the biases of batch normalization layers instead of convolutional weights to increase the number of activations and, in turn, increase the energy consumption.

7 CONCLUSIONS AND FUTURE WORK

This work proposes a novel sponge attack on deep neural networks. The SkipSponge attack changes the parameters of the pre-trained model. We enable our attack to be powerful (increasing energy consumption) and stealthy (making the detection more difficult). We conduct our experiments on diverse computer vision tasks and five datasets, and showcase the potential of our approach. For future work, there are several interesting directions to follow. Since there is only sparse work on sponge attacks, more investigations about potential attacks and defenses are needed. Next, our attack relies on the ReLU activation function that promotes sparsity in

⁶A two-tailed hypothesis test is used to show whether the sample mean is significantly greater than and significantly less than the mean of a population.

neural networks. However, there are other (granted, much less used) activation functions that could potentially bring even more sparsity [4, 23]. Investigating the attack performance for those settings would be then interesting. Lastly, in this work, we used an ASIC accelerator simulator as provided by [44]. Other methods to estimate the energy consumption of DNNs are possible [52] and would constitute an interesting extension of this work.

REFERENCES

- [1] Jorge Albericio, Patrick Judd, Tayler Hetherington, Tor Aamodt, Natalie Enright Jerger, and Andreas Moshovos. Cnvlutin: Ineffectual-neuron-free deep neural network computing. In *2016 ACM/IEEE 43rd Annual International Symposium on Computer Architecture (ISCA)*, pages 1–13, 2016.
- [2] Mostafa Rahimi Azghadi, Corey Lammie, Jason K. Eshraghian, Melika Payvand, Elisa Donati, Bernabé Linares-Barranco, and Giacomo Indiveri. Hardware implementation of deep network accelerators towards healthcare and biomedical applications. *IEEE Transactions on Biomedical Circuits and Systems*, 14(6):1138–1159, 2020.
- [3] Pierre Baldi. Autoencoders, unsupervised learning, and deep architectures. In *Proceedings of ICML workshop on unsupervised and transfer learning*, pages 37–49, 2012.
- [4] Paschalis Bizopoulos and Dimitrios Koutsouris. Sparsely activated networks. *IEEE Transactions on Neural Networks and Learning Systems*, 32(3):1304–1313, March 2021.
- [5] Yu-Hsin Chen, Tushar Krishna, Joel S. Emer, and Vivienne Sze. Eyeriss: An energy-efficient reconfigurable accelerator for deep convolutional neural networks. *IEEE Journal of Solid-State Circuits*, 52(1):127–138, 2017.
- [6] Yunje Choi, Minje Choi, Munyoung Kim, Jung-Woo Ha, Sunghun Kim, and Jaegul Choo. Stargan: Unified generative adversarial networks for multi-domain image-to-image translation. In *2018 IEEE/CVF Conference on Computer Vision and Pattern Recognition*, pages 8789–8797, 2018.
- [7] Yunje Choi, Youngjung Uh, Jaejun Yoo, and Jung-Woo Ha. Stargan v2: Diverse image synthesis for multiple domains. In *Proceedings of the IEEE Conference on Computer Vision and Pattern Recognition*, 2020.
- [8] Antonio Emanuele Cinà, Ambra Demontis, Battista Biggio, Fabio Roli, and Marcello Pelillo. Energy-latency attacks via sponge poisoning. *ArXiv*, abs/2203.08147, 2022.
- [9] Jonathan Frankle and Michael Carbin. The lottery ticket hypothesis: Finding sparse, trainable neural networks, 2019.
- [10] Matt Fredrikson, Somesh Jha, and Thomas Ristenpart. Model inversion attacks that exploit confidence information and basic countermeasures. In *Proceedings of the 22nd ACM SIGSAC conference on computer and communications security*, pages 1322–1333, 2015.
- [11] Xavier Glorot, Antoine Bordes, and Yoshua Bengio. Deep sparse rectifier neural networks. In Geoffrey Gordon, David Dunson, and Miroslav Dudik, editors, *Proceedings of the Fourteenth International Conference on Artificial Intelligence and Statistics*, volume 15 of *Proceedings of Machine Learning Research*, pages 315–323, Fort Lauderdale, FL, USA, 11–13 Apr 2011. PMLR.
- [12] Tianyu Gu, Brendan Dolan-Gavitt, and Siddharth Garg. Badnets: Identifying vulnerabilities in the machine learning model supply chain. *arXiv preprint arXiv:1708.06733*, 2017.
- [13] Song Han, Xingyu Liu, Huizi Mao, Jing Pu, Ardavan Pedram, Mark A. Horowitz, and William J. Dally. Eie: Efficient inference engine on compressed deep neural network, 2016.
- [14] Kaiming He, Xiangyu Zhang, Shaoqing Ren, and Jian Sun. Deep residual learning for image recognition. In *Proceedings of the IEEE conference on computer vision and pattern recognition*, pages 770–778, 2016.
- [15] Sanghyun Hong, Nicholas Carlini, and Alexey Kurakin. Handcrafted backdoors in deep neural networks. In Alice H. Oh, Alekh Agarwal, Danielle Belgrave, and Kyunghyun Cho, editors, *Advances in Neural Information Processing Systems*, 2022.
- [16] Sebastian Houben, Johannes Stallkamp, Jan Salmen, Marc Schlipsing, and C. Igel. Detection of traffic signs in real-world images: The german traffic sign detection benchmark. *The 2013 International Joint Conference on Neural Networks (IJCNN)*, pages 1–8, 2013.
- [17] Phillip Isola, Jun-Yan Zhu, Tinghui Zhou, and Alexei A. Efros. Image-to-image translation with conditional adversarial networks. In *2017 IEEE Conference on Computer Vision and Pattern Recognition (CVPR)*, pages 5967–5976, 2017.
- [18] Matthew Jagielski, Nicholas Carlini, David Berthelot, Alex Kurakin, and Nicolas Papernot. High accuracy and high fidelity extraction of neural networks. In *29th USENIX security symposium (USENIX Security 20)*, pages 1345–1362, 2020.
- [19] Dongyoung Kim, Junwhan Ahn, and Sungjoo Yoo. A novel zero weight/activation-aware hardware architecture of convolutional neural network. In *Proceedings of the Conference on Design, Automation & Test in Europe, DATE '17*, page 1466–1471, Leuven, BEL, 2017. European Design and Automation Association.
- [20] Alex Krizhevsky, Geoffrey Hinton, et al. Learning multiple layers of features from tiny images. 2009.
- [21] Alex Krizhevsky, Ilya Sutskever, and Geoffrey E. Hinton. Imagenet classification with deep convolutional neural networks. In *Proceedings of the 25th International Conference on Neural Information Processing Systems - Volume 1, NIPS'12*, page 1097–1105, Red Hook, NY, USA, 2012. Curran Associates Inc.
- [22] Ram Shankar Siva Kumar, David O'Brien, Kendra Albert, Salomé Viljón, and Jeffrey Snover. Failure modes in machine learning systems. *arXiv preprint arXiv:1911.11034*, 2019.
- [23] Mark Kurtz, Justin Kopinsky, Rati Gelashvili, Alexander Matveev, John Carr, Michael Goin, William Leiserson, Sage Moore, Nir Shavit, and Dan Alistarh. Inducing and exploiting activation sparsity for fast inference on deep neural networks. In Hal Daumé III and Aarti Singh, editors, *Proceedings of the 37th International Conference on Machine Learning*, volume 119 of *Proceedings of Machine Learning Research*, pages 5533–5543. PMLR, 13–18 Jul 2020.
- [24] Ya Le and Xuan Yang. Tiny imagenet visual recognition challenge. *CS 231N*, 7(7):3, 2015.
- [25] Yann LeCun, Corinna Cortes, and CJ Burges. The mnist handwritten digit database. *ATT Labs [Online]*. Available: <http://yann.lecun.com/exdb/mnist>, 2, 2010.
- [26] Kang Liu, Brendan Dolan-Gavitt, and Siddharth Garg. Fine-pruning: Defending against backdooring attacks on deep neural networks. In *Research in Attacks, Intrusions, and Defenses*, page 273–294. Springer International Publishing, 2018.
- [27] Ziwei Liu, Ping Luo, Xiaoqiang Wang, and Xiaoou Tang. Deep learning face attributes in the wild. In *Proceedings of International Conference on Computer Vision (ICCV)*, December 2015.
- [28] Raju Machupalli, Masum Hossain, and Mrinal Mandal. Review of asic accelerators for deep neural network. *Microprocessors and Microsystems*, 89:104441, 2022.
- [29] Mehdi Mirza and Simon Osindero. Conditional generative adversarial nets, 2014.
- [30] Mehdi Mirza and Simon Osindero. Conditional generative adversarial nets. *CoRR*, abs/1411.1784, 2014.
- [31] Iman Mirzadeh, Keivan Alizadeh, Sachin Mehta, Carlo C Del Mundo, Oncel Tuzel, Golnoosh Samei, Mohammad Rastegari, and Mehrdad Farajtabar. Relu strikes back: Exploiting activation sparsity in large language models, 2023.
- [32] B. K. Natarajan. Sparse approximate solutions to linear systems. *SIAM Journal on Computing*, 24(2):227–234, 1995.
- [33] Miloš Nikolić, Mostafa Mahmoud, and Andreas Moshovos. Characterizing sources of ineffectual computations in deep learning networks. In *2018 IEEE International Symposium on Workload Characterization (IISWC)*, pages 86–87, 2018.
- [34] Michael R. Osborne, Brett Presnell, and Berwin A. Turlach. On the lasso and its dual. *Journal of Computational and Graphical Statistics*, 9:319 – 337, 2000.
- [35] Angshuman Parashar, Minsoo Rhu, Anurag Mukkara, Antonio Puglielli, Rangharajan Venkatesan, Brucek Khailany, Joel Emer, Stephen W. Keckler, and William J. Dally. Scnn: An accelerator for compressed-sparse convolutional neural networks. In *2017 ACM/IEEE 44th Annual International Symposium on Computer Architecture (ISCA)*, pages 27–40, 2017.
- [36] Angshuman Parashar, Minsoo Rhu, Anurag Mukkara, Antonio Puglielli, Rangharajan Venkatesan, Brucek Khailany, Joel Emer, Stephen W. Keckler, and William J. Dally. Scnn: An accelerator for compressed-sparse convolutional neural networks, 2017.
- [37] David Patterson, Jeffrey M. Gilbert, Marco Gruteser, Efrén Robles, Krishna Sekar, Yong Wei, and Tenghui Zhu. Energy and emissions of machine learning on smartphones vs. the cloud. *Commun. ACM*, 67(2):86–97, jan 2024.
- [38] David Patterson, Joseph Gonzalez, Quoc Le, Chen Liang, Lluís-Miquel Munguia, Daniel Rothchild, David So, Maud Texier, and Jeff Dean. Carbon emissions and large neural network training, 2021.
- [39] Souvik Paul and Nicolas Kourtellis. Sponge ml model attacks of mobile apps. In *Proceedings of the 24th International Workshop on Mobile Computing Systems and Applications, HotMobile '23*, page 139, New York, NY, USA, 2023. Association for Computing Machinery.
- [40] David E Rumelhart, Geoffrey E Hinton, and Ronald J Williams. Learning internal representations by error propagation. Technical report, California Univ San Diego La Jolla Inst for Cognitive Science, 1985.
- [41] Siddharth Samsi, Dan Zhao, Joseph McDonald, Baolin Li, Adam Michaleas, Michael Jones, William Bergeron, Jeremy Kepner, Devesh Tiwari, and Vijay Gadepally. From words to watts: Benchmarking the energy costs of large language model inference, 2023.
- [42] Avishag Shapira, Alon Zolfi, Luca Demetrio, Battista Biggio, and Asaf Shabtai. Phantom sponges: Exploiting non-maximum suppression to attack deep object detectors. In *2023 IEEE/CVF Winter Conference on Applications of Computer Vision (WACV)*, pages 4560–4569, 2023.
- [43] Reza Shokri, Marco Stronati, Congzheng Song, and Vitaly Shmatikov. Membership inference attacks against machine learning models. In *2017 IEEE symposium on security and privacy (SP)*, pages 3–18. IEEE, 2017.
- [44] Iliia Shumailov, Yiren Zhao, Daniel Bates, Nicolas Papernot, Robert Mullins, and Ross Anderson. Sponge examples: Energy-latency attacks on neural networks. In *2021 IEEE European Symposium on Security and Privacy (EuroS&P)*, pages 212–231,

- 2021.
- [45] Karen Simonyan and Andrew Zisserman. Very deep convolutional networks for large-scale image recognition. *arXiv preprint arXiv:1409.1556*, 2014.
 - [46] Christian Szegedy, Wojciech Zaremba, Ilya Sutskever, Joan Bruna, Dumitru Erhan, Ian Goodfellow, and Rob Fergus. Intriguing properties of neural networks. *arXiv preprint arXiv:1312.6199*, 2013.
 - [47] Dmitrii Torbunov, Yi Huang, Huan-Hsin Tseng, Haiwang Yu, Jin Huang, Shinjae Yoo, Meifeng Lin, Brett Viren, and Yihui Ren. Uvcgan v2: An improved cycle-consistent gan for unpaired image-to-image translation, 2023.
 - [48] Dmitrii Torbunov, Yi Huang, Haiwang Yu, Jin Huang, Shinjae Yoo, Meifeng Lin, Brett Viren, and Yihui Ren. Uvcgan: Unet vision transformer cycle-consistent gan for unpaired image-to-image translation. In *2023 IEEE/CVF Winter Conference on Applications of Computer Vision (WACV)*, pages 702–712, 2023.
 - [49] Zhou Wang, A.C. Bovik, H.R. Sheikh, and E.P. Simoncelli. Image quality assessment: from error visibility to structural similarity. *IEEE Transactions on Image Processing*, 13(4):600–612, 2004.
 - [50] Zhou Wang, Alan C Bovik, Hamid R Sheikh, and Eero P Simoncelli. Image quality assessment: from error visibility to structural similarity. *IEEE transactions on image processing*, 13(4):600–612, 2004.
 - [51] Zijian Wang, Shuo Huang, Yujin Huang, and Helei Cui. Energy-latency attacks to on-device neural networks via sponge poisoning. In *Proceedings of the 2023 Secure and Trustworthy Deep Learning Systems Workshop, SecTL '23*, New York, NY, USA, 2023. Association for Computing Machinery.
 - [52] Tien-Ju Yang, Yu-Hsin Chen, Joel Emer, and Vivienne Sze. A method to estimate the energy consumption of deep neural networks. In *2017 51st Asilomar Conference on Signals, Systems, and Computers*, pages 1916–1920, 2017.
 - [53] Yonghua Zhang, Hongxu Jiang, Xiaobin Li, Haojie Wang, Dong Dong, and Yongxiang Cao. An efficient sparse cnns accelerator on fpga. In *2022 IEEE International Conference on Cluster Computing (CLUSTER)*, pages 504–505, 2022.
 - [54] Min Zhao, Fan Bao, Chongxuan Li, and Jun Zhu. Egsde: Unpaired image-to-image translation via energy-guided stochastic differential equations. In S. Koyejo, S. Mohamed, A. Agarwal, D. Belgrave, K. Cho, and A. Oh, editors, *Advances in Neural Information Processing Systems*, volume 35, pages 3609–3623. Curran Associates, Inc., 2022.
 - [55] Jun-Yan Zhu, Taesung Park, Phillip Isola, and Alexei A. Efros. Unpaired image-to-image translation using cycle-consistent adversarial networks. In *2017 IEEE International Conference on Computer Vision (ICCV)*, pages 2242–2251, 2017.

A GENERATIVE ADVERSARIAL NETWORKS

Generative Adversarial Networks (GANs) are a powerful class of neural networks used for unsupervised learning. GANs comprise two neural networks: a discriminator and a generator. They use adversarial training to produce artificial data identical to actual data. Many popular image translation approaches such as cGAN [17], CycleGAN [55], and StarGAN [6] utilize a combination of loss terms in the objective functions to train the generator and discriminator components. Of these, StarGAN [6] is the most successful, as it can learn multiple attribute translations with only one model. The authors use a combination of three loss terms. First, to make the generated images as real as possible, they adopt an adversarial loss L_{adv} that represents the discriminator’s ability to distinguish the generated images. Second, both components contain a domain classification loss. For the generator component, the classification loss $\lambda_{cls} L_{cls}^f$ of the generated sample needs to be minimized to produce realistic images. For the discriminator component, the classification loss $\lambda_{cls} L_{cls}^r$ for real images and their real attributes needs to be minimized such that the discriminator learns good feature representations of real images. Third, the reconstruction loss L_{rec} is used to train the generator only to change the specified attribute while preserving the rest of the image. The L_{rec} is minimized and calculated by first generating a fake image and subsequently using the generator again to reconstruct the fake image back to its original class. A low L_{rec} represents a small difference between the original image and the reconstructed image, measured with the ℓ_1 norm.

Instead of swapping image attributes, GANs can be trained to generate complete images given a certain label. A well-known architecture is the conditional version of a GAN, called CGAN [29]. This CGAN model can generate MNIST digits by conditioning the generator and discriminator on a given class label during training. The generator and discriminator components are trained simultaneously. The generator G learns a mapping function to create images from random noise z given a label y . G minimizes the loss $\log(1 - D(z | y))$. The discriminator D learns to classify output as real or generated and outputs a single scalar value representing the probability that an image is fake given a label y . D minimizes the loss $\log(D(x | y))$.

B AUTOENCODERS

Autoencoders were first introduced in the 1980s by Hinton and the PDP group [40] to address the problem of “backpropagation without a teacher”. Differing from other neural network architectures that map the relationship between the inputs and the labels, an autoencoder transforms inputs into outputs with the least possible amount of distortion [3]. An autoencoder consists of two parts: encoder (ϕ) and decoder (ψ). The goal of the encoder is to transfer the input to its latent space \mathcal{F} , i.e., $\phi : \mathcal{X} \rightarrow \mathcal{F}$. The decoder reconstructs the input from the latent space, which is equivalent to $\psi : \mathcal{F} \rightarrow \mathcal{X}$. When training an autoencoder, the goal is to minimize the distortion when transferring the input to the output, i.e., the most representative input features are forced to be kept in the smallest layer in the network.

Conditional Generative Adversarial Networks (CGANs) [30] represent a variant of the GAN architecture incorporating additional information to guide the generation process. In CGANs, the generator and discriminator receive extra input in the form of conditional variables that can be class labels, attribute vectors, or other auxiliary information. This conditioning allows for the generation of more targeted and controlled outputs. Then, by providing specific conditions, such as a particular class label, a CGAN can produce images or data samples that conform to desired characteristics.

C SSIM

Wang et al. proposed a measure called structural similarity index (SSIM) that compares local patterns of pixel intensities [50]. SSIM computes the changes between two windows:

$$SSIM(x, \hat{x}) = \frac{(2\mu_x\mu_{\hat{x}} + c_1)(2\sigma_{x\hat{x}} + c_2)}{(\mu_x^2 + \mu_{\hat{x}}^2 + c_1)(\sigma_x^2 + \sigma_{\hat{x}}^2 + c_2)},$$

where μ_x is the pixel sample mean of x , $\mu_{\hat{x}}$ is the pixel sample mean of \hat{x} , c_1 and c_2 are two variables to stabilize the division, σ_x is the variance of x , $\sigma_{\hat{x}}$ is the variance of \hat{x} , and $\sigma_{x\hat{x}}$ is the covariance of x and \hat{x} .

D RELU VS. LEAKYRELU

Table 8 contains the percentage of energy ratio increase and energy ratio of SkipSponge on VGG16 with ReLU as activation layers versus LeakyReLU as activation layers. The energy ratio is the ratio between the average case and the worst case, as described in Section 2. As can be seen, the ratio for the clean model is already at 1.0 before any attack has been performed, meaning there is no sparsity.

